

Modelling of gaseous methylamines in the global atmosphere: Impacts of oxidation and aerosol uptake

Fangqun Yu* and Gan Luo

Atmospheric Sciences Research Center, State University of New York, 251 Fuller Road, Albany,
New York 12203, USA

*corresponding author: fyu@albany.edu

Abstract. Gaseous amines have attracted increasing attention due to their potential role in enhancing particle nucleation and growth and affecting secondary organic aerosol formation. Here we study with a chemistry transport model the global distributions of the most common and abundant amines in the air: monomethylamine (MMA), dimethylamine (DMA), and trimethylamine (TMA). We show that gas phase oxidation and aerosol uptakes are dominant sinks for these methylamines. The oxidation alone (i.e., no aerosol uptake) leads to methylamine lifetimes of 5-10 hours in most parts of low and middle latitude regions. The aerosol uptake with uptake coefficient (γ) of 0.03 (corresponding to the uptake by sulfuric acid particles) reduces the lifetime by ~30% over oceans and much more over the major continents, resulting in methylamine lifetime of less than 1-2 hours over central Europe, East Asia, and Eastern US. With the estimated global emission flux, from the reference, our simulations indicate that [DMA] is generally in the range of 0.1 – 2 ppt when $\gamma = 0.03$ and 0.2-10 ppt when $\gamma = 0$ in the model surface layer over major continents, and decreases quickly with altitude. [DMA] over oceans is below 0.05 ppt and over polar regions is below 0.01 ppt. [MMA] is about a factor of ~2.5 higher while [TMA] is a factor of ~ 8 higher than [DMA]. The simulated concentrations of methylamines are substantially lower than the limited observed values available, with normalized

25 mean bias ranging from -57% ($\gamma = 0$) to -88% ($\gamma = 0.03$) for MMA and TMA, and -78% ($\gamma = 0$)
26 to -93% ($\gamma = 0.03$) for DMA.

27

1. Introduction

In recent years, gaseous amines have attracted more attention due to theoretical, laboratory, and field measurements indicating that amines may considerably enhance particle formation and growth (Kurten et al., 2008; Nadykto et al., 2011, 2014; Almeida et al., 2013; Berndt et al., 2010; Zhao et al., 2011; Erupe et al., 2011; Chen et al., 2012; Wang et al., 2010; Yu et al., 2012). Amines are organic compounds and derivatives of ammonia wherein one or more hydrogen atoms are replaced by a substituent such as an alkyl or aryl group. About 150 amines have been identified in the atmosphere; the most common and abundant amines being the low-molecular-weight methylamines like monomethylamine (MMA), dimethylamine (DMA), and trimethylamine (TMA) (Ge et al., 2011a). Concentrations of amines can exceed several parts-per-billion-volume (ppbv) near their sources (Ge et al., 2011a; Schade and Crutzen, 1995) but are expected to be low farther away as a result of their short lifetime due to oxidation by OH (Atkinson et al., 1978) and uptake by particles (Qiu and Zhang, 2013).

While amines are stronger bases than ammonia and ternary $\text{H}_2\text{SO}_4\text{-H}_2\text{O}$ -amine clusters are more stable (Kurten et al., 2008; Nadykto et al., 2011, 2014; Almeida et al., 2013), the relative role of amines versus ammonia in enhancing particle formation in the atmosphere is yet to be determined (Zollner et al., 2012). This is because the concentration of amines in the atmosphere is generally much lower than that of ammonia (by 2-3 orders of magnitude or more) (Ge et al., 2011a; Hanson et al., 2011). Recent measurements taken during the CLOUD (Cosmics Leaving Outdoor Droplets) chamber experiments at CERN (Almeida et al., 2013) indicate that a [DMA] of above ~ 5 parts-per-trillion-volume (pptv) enhances nucleation substantially, but enhancement drops significantly as [DMA] decreases below that level.

In order to determine the contribution of ternary nucleation involving amines to atmospheric particle production, it is critical to know the concentrations of key amines and their variations in the atmosphere. Due to their high reactivity and low concentrations, measurements of gaseous amines in the background atmosphere are very limited (Ge et al., 2011a). Several studies show [DMA] is below 1 pptv in urban areas (Grönberg et al., 1992a, b) while a couple of other studies observed [DMA] around a few pptv in rural and coastal areas (Hanson et al., 2011; VandenBoer et al., 2011, 2012; Van Neste et al., 1987; Gibb et al., 1999). Although TMA is generally more abundant (Ge et al., 2011a), the concentration of TMA needed to substantially enhance nucleation remains to be studied.

In addition to in-situ measurements, numerical modeling is also needed to integrate the various processes controlling amine concentrations and ultimately assess the impact of amines on global nucleation, aerosol properties, and climate. While limited measurements of amines are available, modeling of global amines is basically non-existent. Myriokefalitakis et al. (2010) explored the potential contribution of amines emitted from oceans to the formation of secondary organic aerosols, assuming amines emissions to be one tenth of the oceanic ammonia emissions. Myriokefalitakis et al. (2010) neither considered amines from continental sources nor presented the concentrations of gaseous amines over oceans. In the present work, we aim to simulate the global distributions of gaseous amines in the air with a global chemistry transport model. The key processes controlling amine concentrations (including emission, transport, oxidation, deposition, and aerosol uptake) are considered and the simulated results are compared to the limited measurements available.

The methods of the present study (including sources, sinks, and model representation) are described in Section 2. The modeling results, comparisons with measurements, and sensitivity studies are given in Section 3. Section 4 is the summary and discussion.

2. Methods

2.1. Sources and fluxes

Amines are ubiquitous atmospheric organic bases, and are emitted from a wide range of sources including animal husbandry, biomass burning, motor vehicles, industry, meat cooking, fish processing, sewage treatment and waste incineration, protein degradation, vegetation, soils, and ocean organisms (Ge et al., 2011a). On a global scale, little is known about the flux of most amines, especially various aromatic amines (Ge et al., 2011a). Among about 150 amines identified in the atmosphere, methylamines (MMA, DMA, and TMA) are most common and abundant. Schade and Crutzen (1995) estimated the global emission fluxes of MMA, DMA, and TMA to be 83 ± 26 , 33 ± 19 , and 169 ± 33 Gg N yr⁻¹, respectively. The total methylamine flux of 285 ± 78 Gg N yr⁻¹ is more than two orders of magnitude smaller than the estimated global ammonia flux of 50000 ± 30000 Gg N yr⁻¹ (Schade and Crutzen, 1995).

2.2. Sinks

The main sinks of amines emitted into the atmosphere include dry and wet deposition, gas phase reactions, and heterogeneous uptake. Since most of the amines are highly soluble, wet deposition is an important process to bring amines in the air to the surface. As organic compounds, gaseous amines undergo oxidation reactions with OH, NO_x, or O₃ (Nielsen et al., 2012; Lee and Wexler, 2013). The lifetimes of amines with respect to OH oxidation are typically a couple of hours, much shorter than those by reactions with O₃ and NO_x. The gaseous

methylamines, which are strong bases, may also undergo rapid acid-base reactions to form salt particles in the presence of inorganic acids (HCl, HNO₃, H₂SO₄) (Murphy et al., 2007). In addition, amines may react with organic acids to form amides (Barsanti and Pankow, 2006). A detailed discussion of the chemistry of amines in the atmosphere can be found in several recent review articles (Nielsen et al., 2012; Lee and Wexler, 2013).

Owing to their high aqueous solubility and strong basicity, gaseous amines can efficiently enter into a particulate phase via direct dissolution and acid-base reactions. The importance of amines with regard to gas/particle partitioning has been supported by the reactive uptake of TMA into ammonium nitrate particles (Lloyd et al., 2009) and amine exchange into ammonium bisulfate and nitrate nuclei (Bzdek et al., 2010). Laboratory studies show that heterogeneous reactions of gaseous alkylamines on H₂SO₄ nanoparticles resulted in the formation of alkyl ammonium sulfates and particle growth (Wang et al., 2010a, b). It has also been observed that methylamine could react with glyoxal in drying cloud droplets to form SOA (De Haan et al., 2009a) and stable aminium salts could be formed by amine and organic acids in the aerosols (Williams et al., 2010). The thermodynamic properties of amines that control their partitioning between the gas and the particle phase in the atmosphere are examined in a review paper (Ge et al., 2011b). An overview of laboratory progress in the multiphase chemistry of amines can be found in Qiu and Zhang (2013).

2.3. Model representation

A numerical model is needed to integrate the various processes influencing the concentrations of amines in the atmosphere. In the present study, we employ GEOS-Chem, a global 3-D model of atmospheric composition driven by assimilated meteorological data from the NASA Goddard Earth Observing System 5 (GEOS-5) (e.g., Bey et al., 2001). The GEOS-

Chem model has been developed and used by many research groups and contains a number of state-of-the-art modules treating various chemical and aerosol processes with up-to-date key emission inventories (for details, see the model webpage <http://geos-chem.org/>). Global ammonia emissions are based on the inventory developed by the Global Emission Inventory Activity (GEIA) (Bouwman et al., 1997) and national emission estimates are used for the US (NEI05), Canada (CAC), Europe (EMEP), and East Asia (Streets2000). While ammonia is simulated in detail in GEOS-Chem, amines are not considered prior to this study. Here, to represent gas phase methylamines, we add three tracers (MMA, DMA, and TMA) in GEOS-Chem V8.3.2 with an advanced particle microphysics (APM) model incorporated (Yu and Luo, 2009).

There exist large uncertainties in the estimated emission fluxes of amines and detailed emission inventories of amines from various sources are currently not available. In the present study, we use the ratios of methylamines to ammonia fluxes given in Schade and Crutzen (1995) but approximate the spatial distribution and seasonal variations of amine emissions following those of ammonia. Such a first order approximation enables us to simulate the typical concentrations of amines in the global atmosphere. The dry and wet deposition, as well as horizontal and vertical transport of amines, is also considered in GEOS-Chem, following the approaches for ammonia.

In the present study, we only take into account the oxidation of methylamines by OH as the oxidation of amines by NO₃ and O₃ is small. There have been limited measurements of the kinetics of OH reactions with simple alkyl amines (Ge et al., 2011a; Nielsen et al., 2012; Lee and Wexler, 2013). In this study we use the reaction coefficients reported by Carl and Crowley (1998): 1.79×10^{-11} , 6.49×10^{-11} , and 3.58×10^{-11} cm³ molecule⁻¹ s⁻¹, for MMA, DMA, and TMA,

140 respectively. For comparison, the reaction coefficient of NH_3 with OH is $1.6 \times 10^{-13} \text{ cm}^3 \text{ molecule}^{-1} \text{ s}^{-1}$ (Atkinson et al., 1997), more than two orders of magnitude smaller. The uptake of amines by
141 particles is considered, using the particle surface areas calculated from particle size distributions
142 predicted by GEOS-Chem-APM. One key uncertainty about the heterogeneous uptake is the
143 uptake coefficient (γ), defined as the ratio of gas surface collisions that result in loss of the
144 amines onto the surface to the total gas surface collisions. Lloyd et al. (2009) reported a reactive
145 uptake coefficient of 2×10^{-3} for the uptake of TMA by ammonium nitrate aerosols at 20% RH.
146 Wang et al. (2010b) studied the uptake of alkylamines (MMA, DMA and TMA) on sulfuric acid
147 surfaces and found uptake coefficients in the range of $(2.0\text{--}4.4) \times 10^{-2}$. In a laboratory study of
148 the heterogeneous reactions between alkylamines (MMA, DMA and TMA) and ammonium salts
149 (ammonium sulfate and ammonium bisulfate), Qiu et al. (2011) found that, for the three
150 alkylamines, the initial uptake coefficients (γ_0) range from 2×10^{-2} to 3.4×10^{-2} and the steady-state
151 uptake coefficients (γ_{ss}) range from 6.0×10^{-3} to 2.3×10^{-4} and decrease as the number of methyl
152 groups on the alkylamine increases. It is clear from these laboratory studies that the values of γ
153 depend on the particle compositions. The secondary components of particles in the atmosphere
154 (sulfate, nitrate, SOA, and ammonium), which are likely to play an important role in the uptake
155 of amines, are generally internally mixed. The uptake coefficients of amines by these mixed
156 particles, under different atmospheric conditions (especially RH), are not yet known. In the
157 present study, the sensitivity of predicted amine concentrations to γ values ranging from 0 (no
158 uptake) to 0.03 is studied. We assume no uptake of amines by pure dust, black carbon, and
159 primary organic carbon. We do not consider the uptake of amines by sea salt particles due to lack
160 of information with regard to the uptake coefficients. The gaseous phase reactions of amines
161 with HNO_3 , HCl , and organic acids are not considered, since oxidation and aerosol uptake likely
162

dominate the loss of amines. In the present study, we also do not consider the re-evaporation of amines after uptake by secondary particles as laboratory studies indicate that amines can react with various acids to form stable aminium salts (e.g., Qiu and Zhang, 2013). For example, recent laboratory measurements show that sulfate particles act as an almost perfect sink (negligible evaporation) for amines (Almeida et al., 2013).

3. Results

The results presented below are based on a one-year simulation (10/2005-12/2006, with the first 3 months as spin-up) using GEOS-Chem v8-03-02 + APM, with the kinetic condensation of low volatile secondary organic gases from successive oxidation aging taken into account (Yu, 2011). The horizontal resolution (latitude by longitude) is $2^\circ \times 2.5^\circ$ and there are 47 vertical layers in the model (surface to 0.01 hpa).

Table 1 shows global annual mean emissions, sinks (due to oxidation, uptake, and dry/wet deposition), and burdens for ammonia, MMA, DMA, and TMA. Sinks and burdens of methylamines under four different uptake coefficients ($\gamma = 0.03, 0.01, 0.001$, and 0) are given. Global ammonia emission flux for 2006 based on GEOS-Chem is $5.8 \times 10^4 \text{ Gg N yr}^{-1}$, about 15% higher than the estimation of Schade and Crutzen (1995). The MMA, DMA, and TMA emissions fluxes assumed in the present study (96.2, 38.3, and 196.0 Gg N yr^{-1} , respectively) are also 15% higher, as the same ratios of methylamines to ammonia emission fluxes given in Schade and Crutzen (1995) are used. The 15% difference is within the estimated methylamines emissions uncertainty of $\sim 30\%$ (Schade and Crutzen, 1995).

As an example for the spatial distribution of emission fluxes, Figure 1 presents the horizontal distributions of DMA emissions assumed in the present study. As mentioned earlier, we

approximate the spatial distribution and seasonal variations of methylamines emissions following those of ammonia. Again, this should be considered as a first order approximation, as the emission rates of amines from various sources may be quite different from those of ammonia. With the understanding of this limitation, we can see from Figure 1 that DMA emission rates are in the range of ~ 0.2 to $10 \text{ kg N km}^{-2}\text{yr}^{-1}$ over major continents and below $0.2 \text{ kg N km}^{-2}\text{yr}^{-1}$ over oceans. For MMA and TMA, the absolute emission fluxes are a factor of 2.5 and 5.1 higher (Table 1). In Figure 1 we also marked the locations of sites where some kind of methylamines measurements are available, as summarized in Table 2. It should be noted that sites A, B, D, and G are close to each other and overlap in Figure 1. Similarly, sites E and F overlap in Fig. 1. Sites J and K are the same location but measurements were taken during different time periods. A comparison of simulated and observed methylamines concentrations is discussed later.

It can be seen from Table 2 that gas phase oxidation and aerosol uptakes are dominant sinks for methylamines (Table 2). As expected, the uptake sinks are sensitive to uptake coefficients (γ) when $\gamma > \sim 0.001$ and the oxidation becomes more important when γ is smaller. The change of γ from 0.03 to 0.001 increases the modeled global burdens of methylamines by a factor of ~ 2.7 . Further decreases of γ from 0.001 to 0 has relatively small effects on the predicted burdens. Dry and wet deposition accounts for 11-14% and 25-35% of the sinks when $\gamma=0.03$ and $\gamma=0$, respectively. The global burdens of MMA, DMA, and TMA are respectively from 0.07 to 0.27 Gg N, 0.03 to 0.08 Gg N, and 0.24 to 0.72 Gg N as γ changes from 0.03 to 0. The ratios of ammonia burden to that of methylamines (MMA+DMA+TMA) range from 74 ($\gamma=0$) to 236 ($\gamma=0.03$). The burdens are roughly but not strictly proportional to emission fluxes because of the difference in the oxidation rates and deposition velocities (which also depend on molecular weights).

Figure 2 shows the simulated horizontal distributions of annual mean DMA oxidation and uptake lifetime (τ , calculated as the ratio of the burden in each grid box to the corresponding sinks associated with oxidation and uptake) and concentration ([DMA]) in the model surface layer (0-150 m above surface) under two aerosol uptake coefficients: (a-b) $\gamma=0$ (i.e., oxidation only) and (c-d) $\gamma=0.03$ (uptake by sulfuric acid particles). The corresponding zonally averaged vertical distributions of τ and [DMA] are given in Figure 3. The oxidation only condition (i.e., no aerosol uptake) leads to a DMA lifetime of 5-10 hours in most parts of lower and middle latitude regions, from the surface to the upper troposphere. The oxidation lifetime is relatively long (from 10 to > 200 hours) over the high latitude regions due to low OH concentrations there. The aerosol uptake with $\gamma=0.03$ (upper limit, corresponding to the uptake by sulfuric acid particles) shortens the lifetime of DMA by ~30% over oceans and much more over the major continents, resulting in a DMA lifetime less than 1-2 hours over central Europe, east Asia, and the eastern US (Fig. 2c). Our sensitivity study indicates that τ values decrease with increasing γ when $\gamma > 0.001$ but become insensitive to γ when $\gamma < 0.001$, as oxidation dominates the lifetime under this condition.

As a result of short lifetime, high values of [DMA] are generally confined to the source regions (Figs. 1, 2b, 2d). Depending on the uptake coefficients, [DMA] in the surface layer over major continents is in the range of 0.1 – 2 ppt when $\gamma = 0.03$ (Fig. 2d) and 0.2-10 ppt when $\gamma = 0$ (Fig. 2b). [DMA] decreases quickly with altitudes, with zonally averaged values dropping below 0.1 ppt a few hundred meters above the surface (Figs. 3b, 3d). [DMA] over oceans are below 0.05 ppt and these DMA are emitted from marine organisms (Fig. 1) rather than transported from continents. [DMA] over polar regions is below 0.01 ppt (Figs. 2 & 3) due to the lack of emissions there (Fig. 1).

The annual mean horizontal and vertical distributions of MMA and TMA concentrations ([MMA], [TMA]) under two γ values (0.03, and 0) are shown in Figures 4 and 5. As a result of same emission spatial distributions (assumed) and short lifetimes, [MMA] and [TMA] have similar spatial distributions as those of [DMA]. [MMA] is generally a factor of ~ 2.5 higher than [DMA], reaching 0.2-5 ppt when $\gamma = 0.03$ (Fig. 4c) and 0.5-20 ppt when $\gamma = 0$ (Fig. 4a) in the surface layer over major continents. While the oxidation rate of MMA is smaller than that of DMA, its deposition velocity is larger. As a result, [MMA] to [DMA] ratio is close to the ratio of the corresponding global emission fluxes. In contrast, both oxidation and deposition velocity of TMA is smaller than those of DMA, leading to a larger [TMA] to [DMA] (~ 8) than the corresponding ratio of emission fluxes (~ 5). [TMA] in the surface layer over major continents reaches 1-10 ppt when $\gamma = 0.03$ (Fig. 5c) and 2-50 ppt when $\gamma = 0$ (Fig. 5a). Similar to [DMA], [MMA] and [TMA] decrease quickly with altitudes, down to < 0.1 ppt above ~ 800 mb (Figs. 4b, 4d, 5b, and 5d).

Figure 6 compares the simulated [MMA], [DMA], and [TMA] with measurements at the sites listed in Table 2 and marked in Fig. 1. The modeling results under four γ values (0.03, 0.01, 0.001, and 0) are given. It should be noted that the model results in Figs. 2-5 are annual mean values, while most of the methylamines data are from various field measurements that lasted from less than one day to a few months (Table 2). Owing to large seasonal variations, model results corresponding to the months of the observations are used for comparisons with observations in Fig. 6. The vertical bars in Fig. 6 (for $\gamma=0.03$ and 0 cases only) define the simulated ranges of monthly mean concentrations of methylamines.

Based on very limited measurements currently available (Table 2), [DMA] in urban areas is smaller than while [MMA] and [TMA] are close to those in rural and coastal areas. Over the

Arabian Sea, measurements of two periods differ by a factor of 5 for [DMA] and by a factor of 10 for [TMA], indicating a large temporal variation in [DMA] and [TMA] concentrations at some locations. It is clear from Figure 6 that the model predictions of methylamines are substantially lower than the limited observed values available, with normalized mean bias (NMB) ranging from -57% ($\gamma = 0$) to -88% ($\gamma = 0.03$) for MMA and TMA, and -78% ($\gamma = 0$) to -93% ($\gamma = 0.03$) for DMA. [MMA] and [TMA] are relatively closer to observed values, especially when $\gamma < 0.001$. It appears that the simulated [DMA] are close to the measured values for the three urban sites (A, B, and C) (Fig. 6b).

It is unclear how much the underestimation is associated with the spatial ($2^\circ \times 2.5^\circ$ model grid box with a depth of ~ 150 m versus measurements at given sites near surface) and temporal (model monthly mean versus measurements of a few days to a few weeks) average. The seasonal variations of simulated concentrations of methylamines are generally within a factor of As we can see from Figs. 2-5 and Table 1, concentrations of methylamines are roughly proportional to the emission fluxes. Methylamines emissions in certain regions could be much larger while, in other regions, much lower than those shown in Fig. 1. Due to the short lifetime of these amines, long range transport is not important, thus the observed amine concentrations can be used to estimate the emission strength in the region. If the measurements are representative and reflect the real methylamines concentrations, the under-prediction of methylamines by one to two orders of magnitude in some sites (Fig. 6) may indicate that the methylamines emissions in these regions are one to two orders of magnitude larger than those assumed in this study (Fig. 1 and Table 1), at least around the sites of the measurements. Apparently long-term measurements of amines at more locations are needed to evaluate the potential importance of amines.

4. Summary and discussion

As a result of the substitution by one or more organic functional groups, amines have stronger basicity than ammonia and may participate in new particle formation in the atmosphere. To integrate the various processes controlling amines concentrations and understand the concentrations of key amines and their spatiotemporal variations in the atmosphere, we simulate the global distributions of amines in the air with a global chemistry transport model (GEOS-Chem), focusing on methylamines (MMA, DMA, and TMA) in this study.

Gas phase oxidation and aerosol uptakes are dominant sinks for methylamines. The uptake sinks are sensitive to uptake coefficients (γ) when $\gamma > \sim 0.001$ and the oxidation becomes more important when γ is smaller. Our simulations show that the oxidation only (i.e., no aerosol uptake) leads to a methylamines lifetime of 5-10 hours in most part of low and middle latitude regions, from the surface to the upper troposphere. The oxidation lifetime is relatively longer (> 10-50 hours) over the high latitude regions due to low OH concentration there. The aerosol uptake with uptake coefficient (γ) of 0.03 (corresponding to the uptake by sulfuric acid particles) reduces the lifetime of methylamines by ~30% over oceans and much more over the major continents, resulting in methylamines lifetime less than 1-2 hours over central Europe, East Asia, and Eastern US. As a result of the short lifetime, high concentrations of methylamines are generally confined to their source regions. Depending on the uptake coefficients, [DMA] in the surface layer over major continents is in the range of 0.1 – 2 ppt when $\gamma = 0.03$ and 0.2-10 ppt when $\gamma = 0$. [DMA] over oceans are below 0.05 ppt and [DMA] over polar regions is below 0.01 ppt. Compared to [DMA], [MMA] is generally a factor of ~2.5 higher while [TMA] is a factor of ~ 8 higher. Concentrations of methylamines decrease quickly with altitudes, with zonally averaged values dropping below 0.1 ppt above the boundary layer.

The simulated concentrations of methylamines are substantially lower than the limited observed values available, with normalized mean bias (NMB) ranging from -57% ($\gamma = 0$) to -88% ($\gamma = 0.03$) for MMA and TMA, and -78% ($\gamma = 0$) to -93% ($\gamma = 0.03$) for DMA. The underestimation can't be explained by the possible uncertainty in the uptake coefficients and long range transport. The concentrations of methylamines are roughly proportional to their emission fluxes, and thus the model under-prediction by one to two orders of magnitude at some sites may indicate that the methylamines emissions in these regions are one to two orders of magnitude higher than those assumed in this study. It should be noted that methylamines measurements are very limited and subject to large uncertainty as well because of its low concentration and short lifetime.

Amines have been suggested to be the most likely compound to sequester carbon dioxide and there exists concern about the potential impacts of substantial increases in future amine emissions (Nielsen et al., 2012). Our study indicates that the impact of amine emissions from carbon sequestration is likely to be local rather than global as a result of their short lifetime. The low concentrations of amines away from source regions (<0.1 - 1 ppt) suggest that the impact of amines on global new particle formation may be quite limited. Nevertheless, amines can exceed a few ppt over the main source regions and thus may substantially enhance new particle formation. It should be noted that about 150 amines have been identified in the atmosphere and amines of different kinds are likely to have different abilities in stabilizing pre-nucleation clusters. It is important to identify those amines with abundant concentrations in the atmosphere and study their ability in enhancing new particle formation. We would like to emphasize that the present global simulations of methylamines are subject to uncertainties associated with emissions, uptake coefficients, and chemistry. Further laboratory study, field measurement, and

numerical modeling are needed to advance our understanding of spatiotemporal distributions of key amines and to evaluate their contributions to new particle formation in the global atmosphere.

Acknowledgments. This study was supported by NASA under grant NNX13AK20G. The GEOS-Chem model is managed by the Atmospheric Chemistry Modeling Group at Harvard University with support from NASA's Atmospheric Chemistry Modeling and Analysis Program.

References

Almeida J, Schobesberger S, Kürten A, Ortega IK, Kupiainen-Määttä O, Praplan AP, Adamov A, Amorim A, Bianchi F, Breitenlechner M, David A, Dommen J, Donahue NM, Downard A, Dunne E, Duplissy J, Ehrhart S, Flagan RC, Franchin A, Guida R, Hakala J, Hansel A, Heinritzi M, Henschel H, Jokinen T, Junninen H, Kajos M, Kangasluoma J, Keskinen H, Kupc A, Kurtén T, Kvashin AN, Laaksonen A, Lehtipalo K, Leiminger M, Leppä J, Loukonen V, Makhmutov V, Mathot S, McGrath MJ, Nieminen T, Olenius T, Onnela A, Petäjä T, Riccobono F, Riipinen I, Rissanen M, Rondo L, Ruuskanen T, Santos FD, Sarnela N, Schallhart S, Schnitzhofer R, Seinfeld JH, Simon M, Sipilä M, Stozhkov Y, Stratmann F, Tomé A, Tröstl J, Tsagkogeorgas G, Vaattovaara P, Viisanen Y, Virtanen A, Vrtala A, Wagner PE, Weingartner E, Wex H, Williamson C, Wimmer D, Ye P, Yli-Juuti T, Carslaw KS, Kulmala M, Curtius J, Baltensperger U, Worsnop DR, Vehkamäki H, Kirkby J.: Molecular understanding of sulphuric acid–amine particle nucleation in the atmosphere, *Nature*, 502, 359-363, 2013.

346 Atkinson, R., Baulch, D.L., Cox, R.A., Hampson Jr., R.F., Kerr, J.A., Rossi, M.J., Troe, J.,:
 347 Evaluated kinetic, photochemical, and heterogeneous data for atmospheric chemistry. V-
 348 IUPAC subcommittee on gas kinetic data evaluation for atmospheric chemistry. Journal of
 349 Physical and Chemical Reference Data 26, 521-1011, 1997.

350 Barsanti, K.C., Pankow, J.F.: Thermodynamics of the formation of atmospheric organic
 351 particulate matter by accretion reactions-part 3: carboxylic and dicarboxylic acids,
 352 Atmospheric Environment, 40, 6676-6686, 2006.

353 Berndt, T., Stratmann, F., Sipilä, M., Vanhanen, J., Petäjä, T., Mikkilä, J., Grüner, A., Spindler,
 354 G., Lee Mauldin III, R., Curtius, J., Kulmala, M., and Heintzenberg, J.: Laboratory study on
 355 new particle formation from the reaction OH + SO₂: influence of experimental conditions,
 356 H₂O vapour, NH₃ and the amine tert-butylamine on the overall process, Atmos. Chem. Phys.,
 357 10, 7101-7116, doi:10.5194/acp-10-7101-2010, 2010.

358 Bey, I., Jacob, D. J., Yantosca, R. M., Logan, J. A., Field, B. D., Fiore, A. M., Li, Q., Liu, H. Y.,
 359 Mickley, L. J., and Schultz M. G.: Global modeling of tropospheric chemistry with
 360 assimilated meteorology: Model description and evaluation, J. Geophys. Res., 106(D19),
 361 23073–23095, doi:10.1029/2001JD000807, 2001.

362 Bouwman, A.F., Lee, D.S., Asman, W.A.H., Dentener, F.J., Van Der Hoek, K.W., Olivier,
 363 J.G.J.: A global high-Å-resolution emission inventory for ammonia, Global Biogeochemical
 364 Cycles, 11, 561-11,587, 1997.

365 Bzdek, B.R., Ridge, D.P., Johnston, M.V.: Amine reactivity with charged sulfuric acid clusters,
 366 Atmos. Chem. Phys., 11: 8735–8743, doi:10.5194/acp-11-8735-2011, 2011.

367 Carl, S.A., Crowley, J.N.: Sequential two(blue) photon absorption by NO₂ in the presence of H₂
 368 as a source of OH in pulsed photolysis kinetic studies: rate constants for reaction of OH with

369 CH_3NH_2 , $(\text{CH}_3)_2\text{NH}$, $(\text{CH}_3)_3\text{N}$, and $\text{C}_2\text{H}_5\text{NH}_2$ at 295 K, Journal of Physical Chemistry A 102,
 370 8131-8141, 1998.

371 Chen, M., Titcombe, M., Jiang, J., Kuang, C., Fischer, M. L., Edgerton, E., Eisele, F. L.,
 372 Siepmann, J. I., Hanson, D. H., Zhao, J., and McMurry, P. H.: Acid-base chemical reaction
 373 model for nucleation rates in the polluted boundary layer, Proc. Nat. Acad. Sci., 109, 18713–
 374 18718, 2012.

375 De Haan, D.O., Tolbert, M.A., Jimenez, J.L.: Atmospheric condensed-phase reactions of glyoxal
 376 with methylamine, Geophysical Research Letters, 36, L11189, 2009.

377 Erupe, ME., Viggiano, AA., Lee, S-H.: The effect of trimethylamine on atmospheric nucleation
 378 involving H_2SO_4 , Atmos. Chem. Phys., 11, 4767-4775, 2011.

379 Ge, X. L., Wexler, A. S., Clegg, S. L.: Atmospheric amines – Part I. A review, Atmos. Environ.,
 380 45, 524–546, 2011a.

381 Ge, X. L., Wexler, A.S., Clegg, S.L.: Atmospheric amines – Part II. Thermodynamic properties
 382 and gas/particle partitioning, Atmospheric Environment, 45, 561-577, 2011b.

383 Gibb, S.W., Mantoura, R.F.C., Liss, P.S.: Ocean-atmosphere exchange and atmospheric
 384 speciation of ammonia and methylamines in the region of the NW Arabian Sea, Global
 385 Biogeochemical Cycles, 13, 161-178, 1999a.

386 Grönberg, L., Lovkvist, P., Jönsson Å, J.: Measurement of aliphatic amines in ambient air and
 387 rainwater, Chemosphere, 24, 1533-1540, 1992a.

388 Grönberg, L., Lovkvist, P., Jönsson Å, J.: Determination of aliphatic amines in air by membrane
 389 enrichment directly coupled to a gas chromatograph, Chromatographia, 33, 77-82, 1992b.

390 Hanson, D. R., McMurry, P. H., Jiang, J., Tanner, D., Huey, L. G.: Ambient pressure proton
 391 transfer mass spectrometry: detection of amines and ammonia, *Environ. Sci. Technol.*, 45,
 392 8881–8888, 2011.

393 Kurten, T., Loukonen, V., Vehkamäki, H., Kulmala, M.: Amines are likely to enhance neutral
 394 and ion-induced sulfuric acid-water nucleation in the atmosphere more effectively than
 395 ammonia, *Atmos. Chem. Phys.*, 8: 4095-4103, 2008.

396 Lee, D., Wexler, A. S.: Atmospheric amines – Part III: Photochemistry and toxicity,
 397 *Atmospheric Environment*, 71, 95-103, 2013.

398 Lloyd, J.A., Heaton, K.J., Johnston, M.V.: Reactive uptake of trimethylamine into ammonium
 399 nitrate particles, *Journal of Physical Chemistry A*, 113, 4840-4843, 2009.

400 Murphy, S. M., Sorooshian, A., Kroll, J. H., Ng, N. L., Chhabra, P., Tong, C., Surratt, J. D.,
 401 Knipping, E., Flagan, R. C., and Seinfeld, J. H.: Secondary aerosol formation from
 402 atmospheric reactions of aliphatic amines, *Atmos. Chem. Phys.*, 7, 2313-2337,
 403 doi:10.5194/acp-7-2313-2007, 2007.

404 Myriokefalitakis, S., Vignati, E., Tsigaridis, K., Papadimas, C., Sciare, J., Mihalopoulos, N.,
 405 Facchini, M. C., Rinaldi, M., Dentener, F. J., Ceburnis, D., Hatzianastasiou, N., O'Dowd, C.
 406 D., van Weele, M., and Kanakidou, M.: Global modelling of the oceanic source of organic
 407 aerosols, *Adv. Meteorol.*, 2010, 939171, doi:10.1155/2010/939171, 2010.

408 Nadykto, A. B., Herb, J., Yu, F., and Xu, Y.: Enhancement due to dimethylamine and large
 409 uncertainties in the thermochemistry of amine-enhanced nucleation in the Earth's atmosphere,
 410 *Chemical Physics Letters*, 10.1016/j.cplett.2014.03.036, 2014.

411 Nadykto, A. B., Yu, F., Yakovleva, M., Herb, J., and Xu, Y.: Amines in the Earth's Atmosphere:
412 A DFT Study of the Thermochemistry of Pre-Nucleation Clusters, *Entropy*, 13, 554-569,
413 2011.

414 Nielsen, C.J., Herrmann, H., Weller, C.: Atmospheric chemistry and environmental impact of the
415 use of amines in carbon capture and storage (CCS), *Chem. Soc. Rev.*, 41, 6684e6704, 2012.

416 Qiu, C., and Zhang, R.: Multiphase chemistry of atmospheric amines, *Phys. Chem. Chem. Phys.*,
417 15, 5738–5752, 2013.

418 Qiu, Q., Wang, L., Lal, V., Khalizov, A.F., and Zhang, R.: Heterogeneous Chemistry of
419 Alkylamines on Ammonium Sulfate and Ammonium Bisulfate, *Environ. Sci. Technol.*, 45,
420 4748–4755, 2011.

421 Schade, G.W., Crutzen, P.J.: Emission of aliphatic amines from animal husbandry and their
422 reactions: potential source of N₂O and HCN, *Journal of Atmospheric Chemistry*, 22, 319-346,
423 1995.

424 Van Neste, A., Duce, R.A., Lee, C.: Methylamines in the marine atmosphere, *Geophysical*
425 *Research Letters*, 7, 711-714, 1987.

426 VandenBoer, T. C., Petroff, A., Markovic, M. Z., and Murphy, J. G.: Size distribution of alkyl
427 amines in continental particulate matter and their online detection in the gas and particle
428 phase, *Atmos. Chem. Phys.*, 11, 4319-4332, doi:10.5194/acp-11-4319-2011, 2011.

429 VandenBoer, T.C., Markovic, M.Z., Petroff, A., Czar, M.F., Borduas, N., Murphy, J.G.: Ion
430 chromatographic separation and quantitation of alkyl methylamines and ethylamines in
431 atmospheric gas and particulate matter using preconcentration and suppressed conductivity
432 detection, *Journal of Chromatography A*, 1252, 74-83, 2012.

433 Wang, L., Khalizov, A. F., Zheng, J., Xu, W., Ma, Y., Lal, V., Zhang, R.: Atmospheric
 434 nanoparticle formed from heterogeneous reactions of organics, *Nat. Geosci.*, 3, 238–242,
 435 2010a.

436 Wang, L., Lal, V., Khalizov, A. F., Zhang, R.: Heterogeneous chemistry of alkylamines with
 437 sulfuric acid: implications for atmospheric formation of alkylaminium sulfates, *Environ. Sci.*
 438 *Technol.*, 44, 2461–2465, 2010b.

439 Williams, B. J., Goldstein, A. H., Kreisberg, N. M., Hering, S. V., Worsnop, D. R.,
 440 Ulbrich, I. M., Docherty, K. S., and Jimenez, J. L.: Major components of atmospheric organic
 441 aerosol in southern California as determined by hourly measurements of source marker
 442 compounds, *Atmos. Chem. Phys.*, 10, 11577–11603, doi:10.5194/acp-10-11577-2010, 2010.

443 Yu, F.: A secondary organic aerosol formation model considering successive oxidation aging and
 444 kinetic condensation of organic compounds: global scale implications, *Atmos. Chem. Phys.*,
 445 11, 1083–1099, doi:10.5194/acp-11-1083-2011, 2011.

446 Yu, F., and Luo, G.: Simulation of particle size distribution with a global aerosol model:
 447 contribution of nucleation to aerosol and CCN number concentrations, *Atmos. Chem. Phys.*,
 448 9, 7691–7710, doi:10.5194/acp-9-7691-2009, 2009.

449 Yu, H., McGraw, R., and Lee S.-H.: Effects of amines on formation of atmospheric sub-3 nm
 450 particles and their subsequent growth, *Geophys. Res. Lett.*, 39, L02807, doi:
 451 10.1021/2011GL050099, 2012.

452 Zhao, J., Smith, J. N., Eisele, F. L., Chen, M., Kuang, C., and McMurry, P. H.: Observation of
 453 neutral sulfuric acid-amine containing clusters in laboratory and ambient measurements,
 454 *Atmos. Chem. Phys.*, 11, 10823–10836, 2011.

455 Zollner, J. H., Glasoe, W. A., Panta, B., Carlson, K. K., McMurry, P. H., and Hanson, D. R.:
456 Sulfuric acid nucleation: power dependencies, variation with relative humidity, and effect of
457 bases, *Atmos. Chem. Phys.*, 12, 4399-4411, doi:10.5194/acp-12-4399-2012, 2012.
458
459
460

461 Table 1. Calculated global annual mean emissions, sinks, and burdens of ammonia, MMA,
 462 DMA, and TMA. Sinks and burdens under four different uptake coefficients ($\gamma = 0.03, 0.01,$
 463 $0.001,$ and 0) are given.

		Emission	Oxidation	Uptake	Dry & Wet Deposition	Burden
	γ	(Gg N/yr)	(Gg N/yr)	(Gg N/yr)	(Gg N/yr)	(Gg N)
Ammonia		5.8×10^4	-4.9×10^2	-3.8×10^4	-1.9×10^4	79.9
MMA	0.03	96.2	-17.2	-65.8	-13.2	0.07
MMA	0.01	96.2	-28.4	-48.1	-19.8	0.12
MMA	0.001	96.2	-51.7	-14.2	-30.4	0.22
MMA	0	96.2	-61.8	0.0	-34.4	0.27
DMA	0.03	38.3	-12.2	-21.9	-4.2	0.03
DMA	0.01	38.3	-17.3	-15.0	-6.0	0.05
DMA	0.001	38.3	-25.9	-3.8	-8.6	0.08
DMA	0	38.3	-28.9	0.0	-9.3	0.08
TMA	0.03	196.0	-49.8	-122.0	-23.9	0.24
TMA	0.01	196.0	-75.4	-85.7	-34.7	0.38
TMA	0.001	196.0	-122.0	-23.0	-50.9	0.63
TMA	0	196.0	-140.0	0.0	-56.2	0.72

464
 465
 466
 467

Table 2. Available measurements of MMA, DMA, and TMA concentrations (in pptv) and site information.

Site information (Latitude, Longitude)	Site Type	Observation period	[MMA]	[DMA]	[TMA]	References
A. Gothenburg, Sweden (57.73, 11.97)	Urban	Aug 24-26, 1991	3.6±0.9	0.7±0.5	1.3±0.6	Grönberg et al. (1992a)
B. Lund, Sweden (55.71, 13.19)	Urban	Jul, 1991	16±5	0.5±0.3	5.2±2	Grönberg et al. (1992b)
C. Atlanta, GA (33.85, -84.41)	Urban	6/23-8/25, 2009	<0.2	0.5 - 2	4 - 15	Hanson et al. (2011)
D. Vallby, Sweden (59.55, 17.13)	Rural	Jul, 1991	10±3	1.8±0.6	41±14	Grönberg et al. (1992b)
E. Toronto, ON (43.67, -79.39)	Rural	6/27-7/5, 2009		0.2 – 2.5		VandenBoer et al. (2011)
F. Egbert, ON (44.23, -79.79)	Agricultural and semi- forested	10/15-11/2, 2010		6.5±2.1	1.0 - 10	VandenBoer et al. (2012)
G. Coastal Sweden (Malmö) (55.62, 13.00)	Coast	Aug 13-15, 1991	4.4±1.1	1.1±0.4	8.7±3.1	Grönberg et al. (1992a)
H. Oahu, Hawaii (21.48, -158.00)	Coast	Jul-Aug, 1985	0.2±0.1	2.0±1.1	0.7±0.4	Van Neste et al. (1987)
I. Narragansett, Rhode Island (41.45, -71.45)	Coast		1.2±0.3	5.3±0.9	2.2±0.9	Van Neste et al. (1987)
J. Arabian Sea (14, 63)	Arabian Sea	8/27-10/4, 1994	2.5	0.9	0.02	Gibb et al. (1999)
K. Arabian Sea (14, 63)	Arabian Sea	11/16-12/19, 1994	3.2	4.4	0.2	Gibb et al. (1999)
L. NW Atlantic (13.2, -66.1)	Marine	2/28/1986	0.33			Mopper and Zika (1987)

Figure Captions

Figure 1. Horizontal distributions of annual mean DMA emissions assumed in the present study.

Figure 2. Simulated horizontal distributions of annual mean DMA lifetime and concentration ([DMA]) in the model surface layer (0-150 m above surface) under two aerosol uptake coefficients: (a-b) $\gamma=0$ (i.e., oxidation only) and (c-d) $\gamma=0.03$ (uptake by sulfuric acid particles).

Figure 3. Same as Fig. 2 but for zonally averaged values. Vertical axis is the ratio of pressure (P) at the model layer to the pressure at the surface (P_{surf}).

Figure 4. Horizontal distributions of [MMA] in the surface layer (a, c) and its zonally averaged values (b, d) under two different uptake coefficients ($\gamma = 0.03$, and 0).

Figure 5. Same as Figure 4 except for [TMA].

Figure 6. A comparison of simulated and measured [MMA], [DMA], and [TMA] at the sites listed in Table 2 and marked in Fig. 1 by letters. Model results correspond to the months of the observations, and vertical bars define the simulated ranges of monthly mean values.

Fig 1

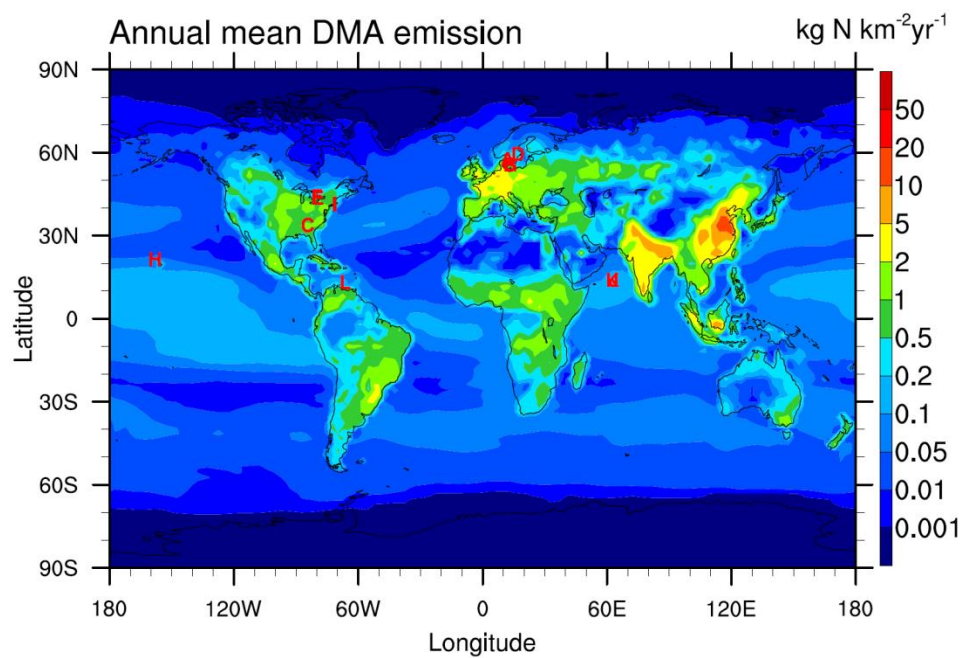


Fig 2

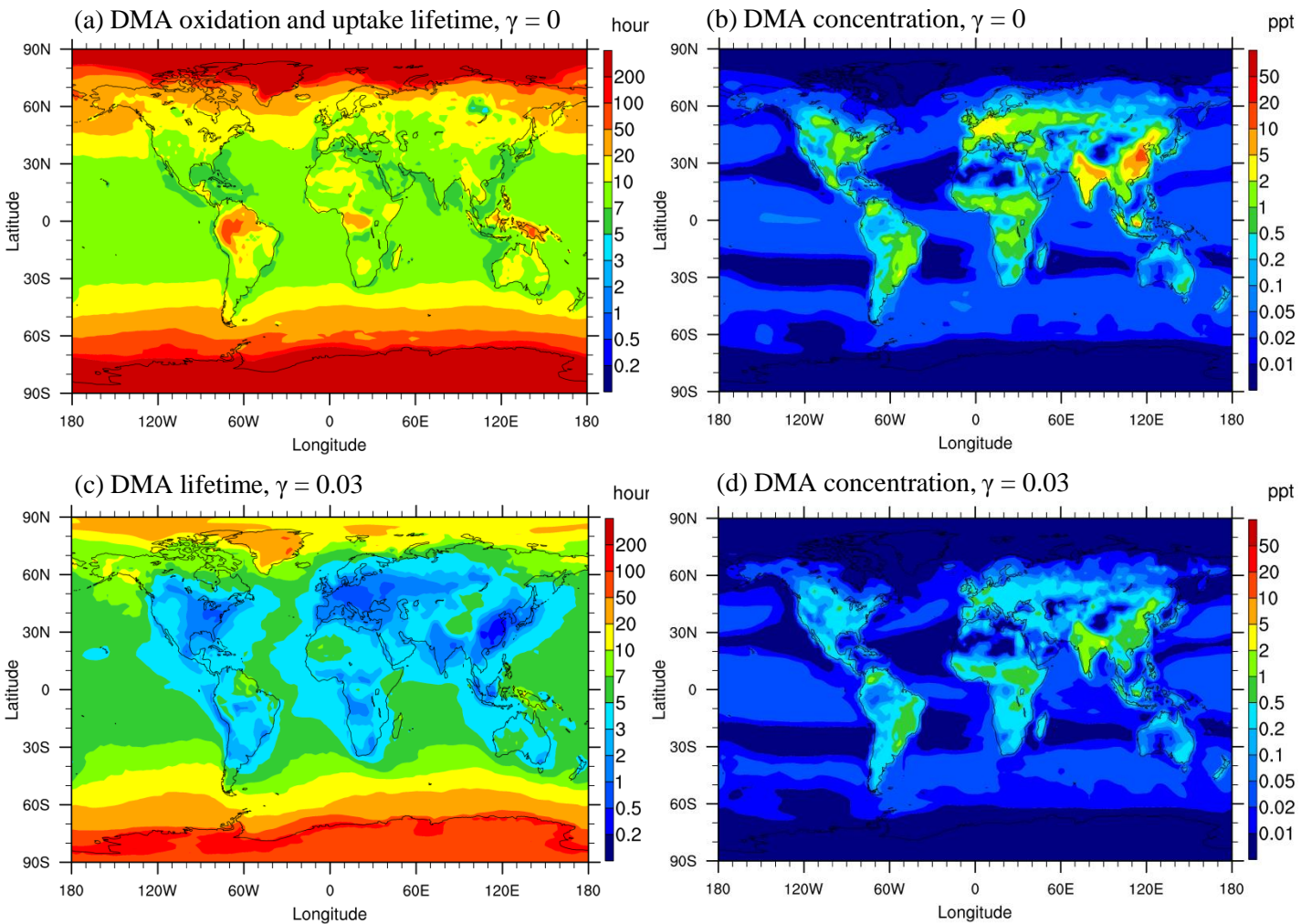


Fig 3

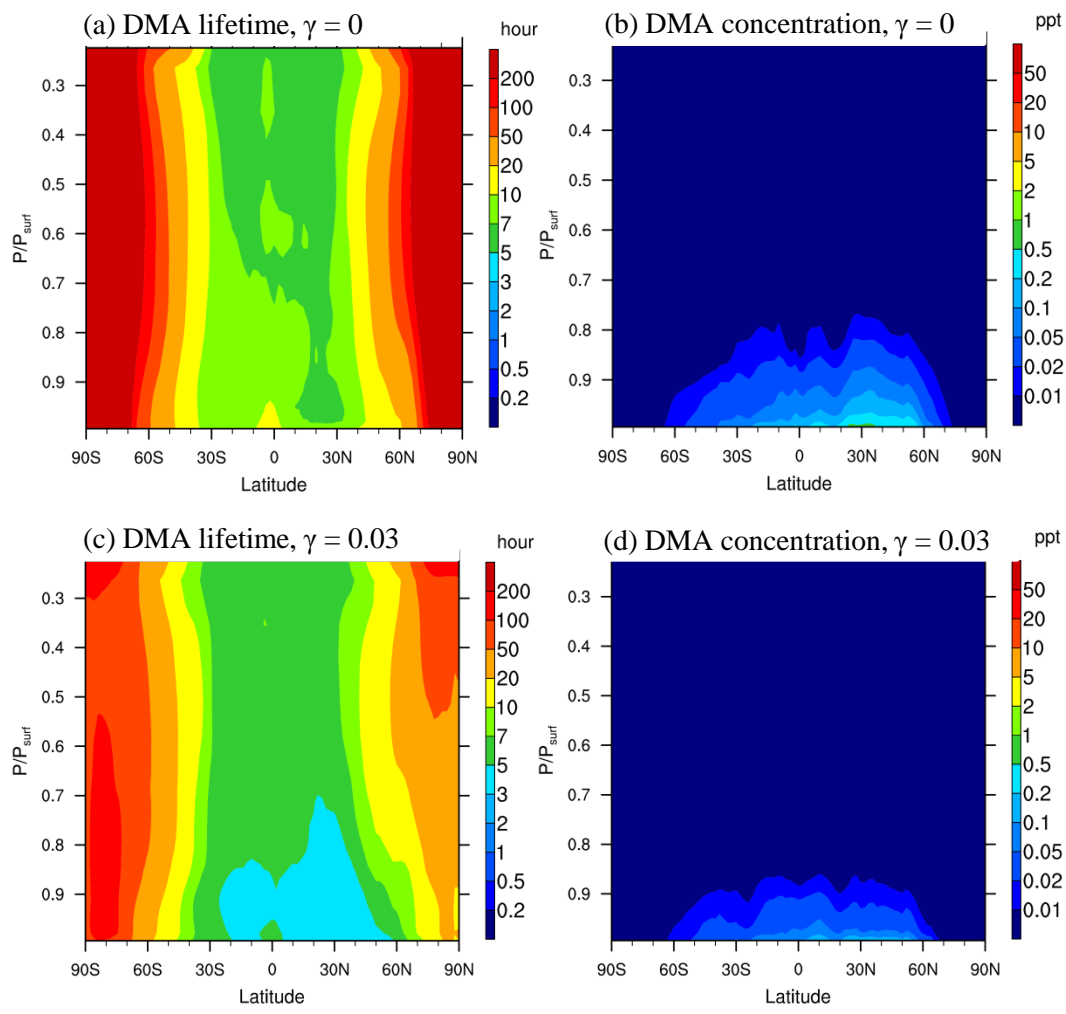


Fig 4

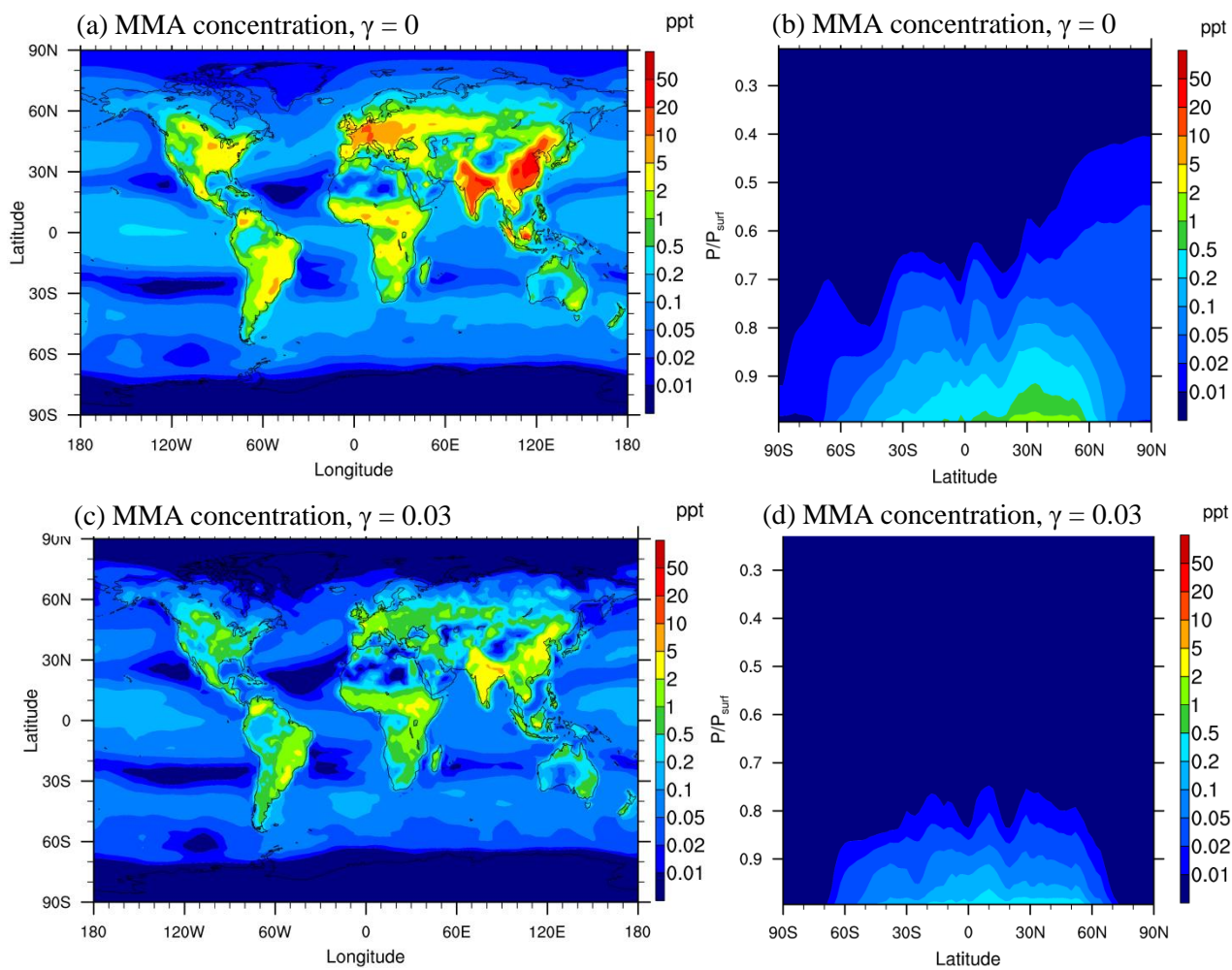


Fig 5

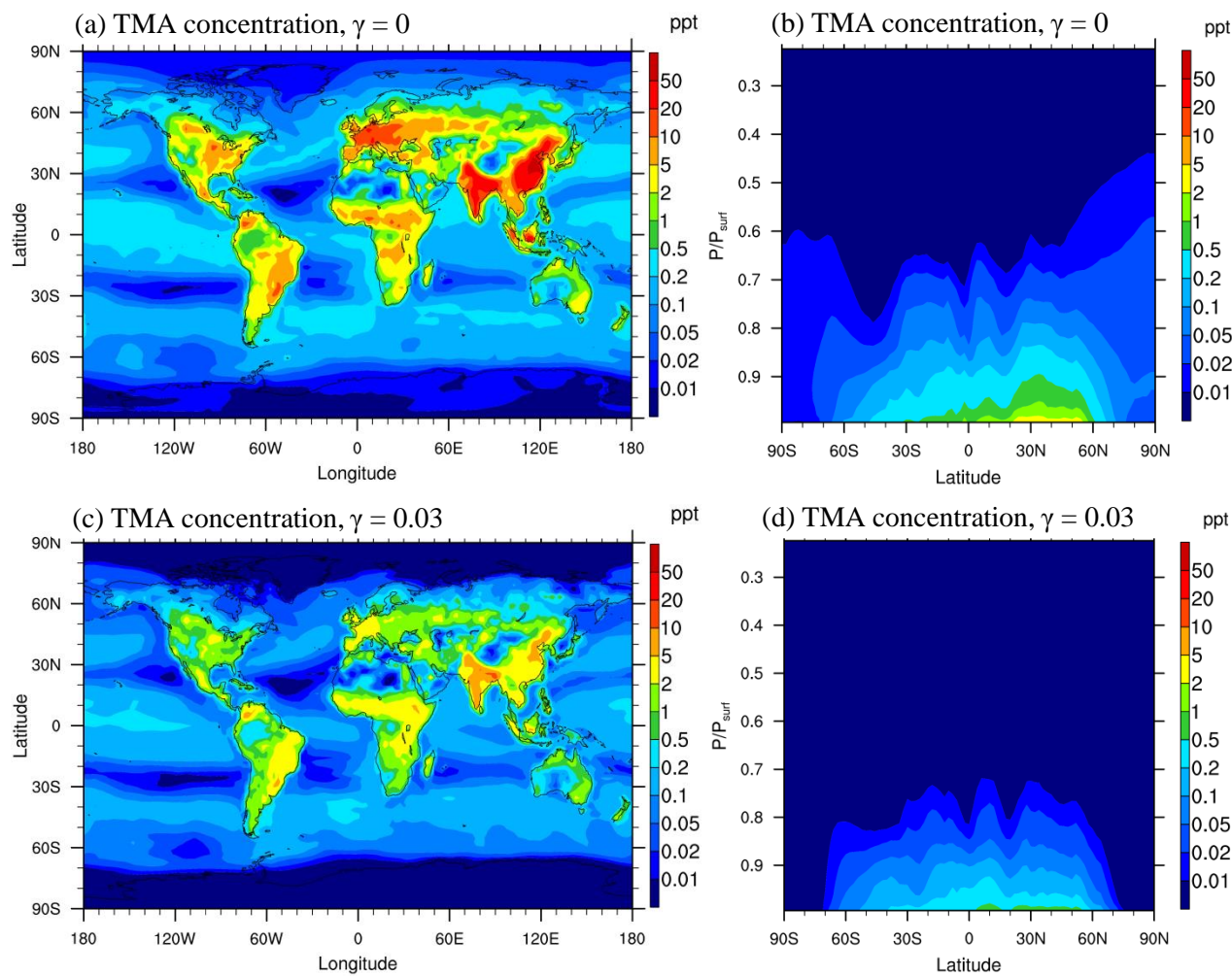


Fig 6

